

Research Article

Research of Impact Load in Large Electrohydraulic Load Simulator

Yongguang Liu, Xiaohui Gao, and Zhongcai Pei

School of Automation Science and Electrical Engineering, Beihang University, Beijing 100191, China

Correspondence should be addressed to Xiaohui Gao; hgaixiaohui@126.com

Received 7 July 2014; Revised 26 July 2014; Accepted 26 July 2014; Published 18 August 2014

Academic Editor: Hui Zhang

Copyright © 2014 Yongguang Liu et al. This is an open access article distributed under the Creative Commons Attribution License, which permits unrestricted use, distribution, and reproduction in any medium, provided the original work is properly cited.

The stronger impact load will appear in the initial phase when the large electric cylinder is tested in the hardware-in-loop simulation. In this paper, the mathematical model is built based on AMESim, and then the reason of the impact load is investigated through analyzing the changing tendency of parameters in the simulation results. The inhibition methods of impact load are presented according to the structural invariability principle and applied to the actual system. The final experimental result indicates that the impact load is inhibited, which provides a good experimental condition for the electric cylinder and promotes the study of large load simulator.

1. Introduction

Electrohydraulic load simulator gets favor of many experts because of its fast response, high precision, good dynamic performance, high power, and interference rejection [1–4]. Since there are many nonlinear factors in the electrohydraulic servo system, such as load disturbance, friction, and asynchronous response, how to overcome them becomes the research focus. Some experts have greatly improved the dynamic response performance of the electrohydraulic system through advanced control algorithm [5–8], but they pay more attention to the dynamic tracking process and ignore the initial stage. The electrohydraulic load simulator is a kind of passive loading way and the extra force will appear due to the asynchronous response of two actuators. Many control methods are proposed to suppress the extra force to improve the dynamic tracing precision [9–16]. These control methods can reduce the amplitude of extra force to some extent, but it is difficult to apply them to the high precision real-time control system because of their complexity. The impact load that is a kind of extra force will appear in the initial phase when electric cylinder is tested in the hardware-in-loop simulation, which seriously reduces the dynamic loading precision and may destroy the electric cylinder. Therefore, it is necessary to research the principle of the

impact load and adopt some simple control methods which can be applied in the high precision real-time control system.

2. Large Electrohydraulic Load Simulator

Large electrohydraulic load simulator is applied to simulate load in the rising process of the missile launcher to test the performance of electric cylinder. This test bed consists of experiment platform, measurement and control system, and hydraulic system, which can provide 100 t (ton) loading force, 100 mm/s velocity, and 0–5 m loading range. 100 t hydraulic servo cylinder, support, rail guided vehicle, and 30 t electric cylinder compose the platform (Figure 1). The LabWindows, that is, a kind of configuration software, is applied to be an upper computer in the measurement and control system, which is applied to issue instructions and display sampling data. The real-time control system adopts RTX whose control period is 1 ms. Hydraulic system can provide 21 MPa pressure and 300 L/min flow. The load response curve of the electrohydraulic load simulator is shown in Figure 2. It can be seen that the impact load is up to 40 t in the initial stages of loading which has been far beyond the limit load of 30 t electric cylinder. Therefore, it is necessary to research the reason and inhibition methods of the impact load.

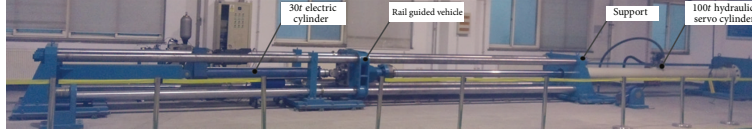


FIGURE 1: Large electrohydraulic load simulator test bed.

TABLE 1: Main parameters of position servo system.

$K_e/(V \cdot (\text{radps})^{-1})$	$K_m/(N \cdot m \cdot A^{-1})$	L_a/H	R_a/Ω	η
1.691	2.7	0.0025	0.058	0.8
$J_b/(\text{kg} \cdot \text{m}^2)$	$f_b/(N \cdot m \cdot (\text{radps})^{-1})$	P_h/m	f_c	
0.012	0.0063	0.02	0.3	
$f_a/(N \cdot m \cdot (\text{radps})^{-1})$	$J_a/(\text{kg} \cdot \text{m}^2)$	i	M_c/kg	
0.0016	0.0495	12	1200	

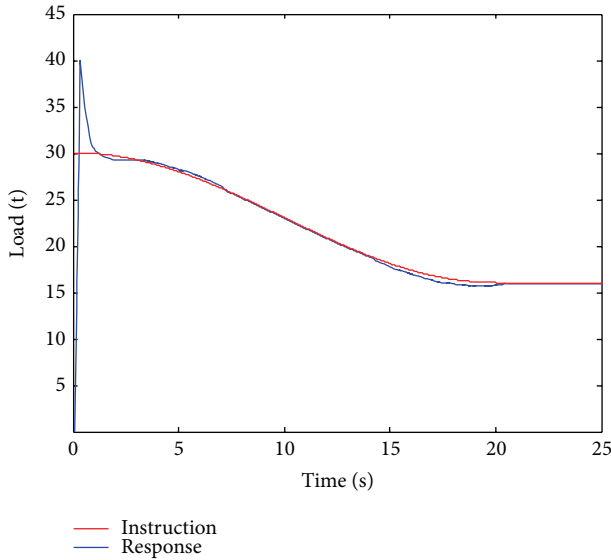


FIGURE 2: Dynamic load response.

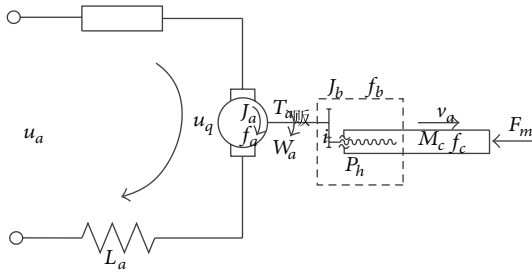


FIGURE 3: Model of electric cylinder.

3. Modeling and Simulation Based on AMESim

The test bed is a synthetic system consisting of mechanism, hydraulic, measurement and control, which can be divided into position servo system and load simulation servo system. Firstly we, respectively, build mathematic model for the servo system based on AMESim. Then the parameters are

set and adjusted to keep consistency between experiment and simulation curve. Finally, we get the mathematic model of the test bed through combining two servo systems. This model will be applied to analyze the reason of the impact load and design controller.

3.1. Modeling and Simulation of the Position Servo System. Position servo system is to control the position of electric cylinder without load. The electric cylinder is composed of servo motor, gear reducer, screw, and piston rod and its transmission model is shown in Figure 3 [16–19]. Equation (1) shows the mathematic model of the position servo system and the block diagram is shown in Figure 4. The main parameters are shown in Table 1. When the position instruction is 100 mm and the load instruction (F_m) is 0 t, the experiment and simulation response curves are shown in Figure 5. It indicates the correctness of this model. Consider

$$\begin{aligned}
 u_a - u_q &= i_a R_a + L_a \frac{di_a}{dt}, \\
 T_a - T_b &= J_a \frac{d^2\theta_a}{dt^2} + f_a \frac{d\theta_a}{dt}, \\
 u_q &= K_e \frac{d\theta_a}{dt}, \\
 T_b - T_m &= J_b \frac{d^2\theta_a}{dt^2} + f_b \frac{d\theta_a}{dt}, \\
 T_m - \frac{F_m P_h}{2\pi\eta i} &= M_c \frac{d^2 l_a}{dt^2} + f_c \frac{dl_a}{dt}, \\
 l_a &= \frac{\theta_a P_h}{2\pi i},
 \end{aligned} \tag{1}$$

where l is the position instruction; w is the rotate speed instruction of servo motor, u_a is the input voltage of the armature winding; i_a is the current of the armature winding; R_a is the resistance of the armature winding; K_m is the electromagnetic torque coefficient; K_e is the voltage coefficient; T_a is the electromagnetic torque of the motor shaft; T_b is the output moment of motor; T_m is the output moment of electric

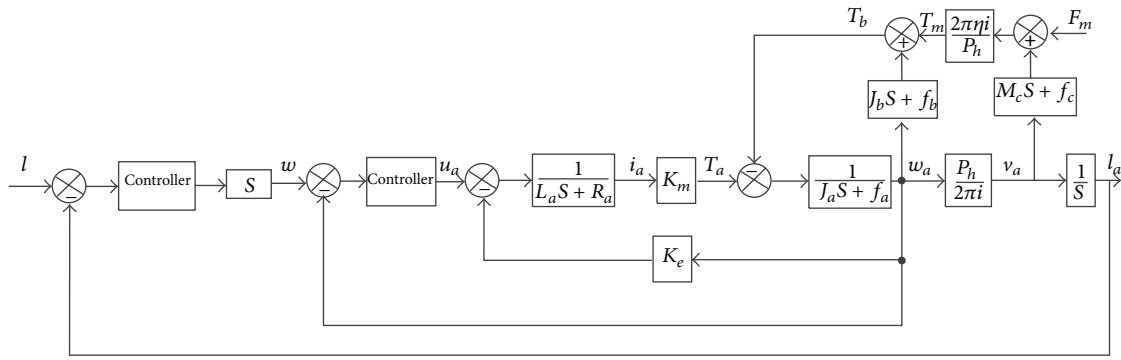


FIGURE 4: Block diagram of position servo system.

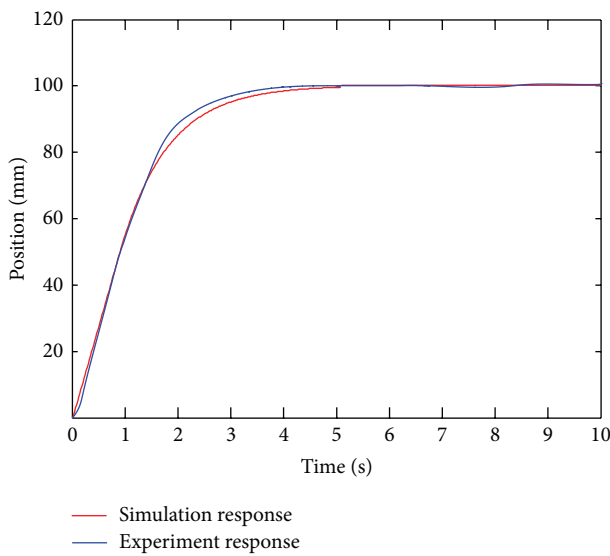


FIGURE 5: Response of the position servo system.

cylinder; J_a is the moment of inertia of the motor shaft; f_a is the viscous friction coefficient of the motor shaft; w_a is the output speed of servo motor; l_a is the position response; J_b is the moment of inertia of the drive system; f_b is the viscous friction coefficient of the drive system; i is the transmission ratio; P_h is the screw lead; η is the mechanical transmission efficiency; M_c is the quality of the piston rod; f_c is the viscous friction coefficient of the piston rod; F_m is the loading force.

3.2. Modeling and Simulation of the Load Simulation Servo System. Load simulation servo system is to control the output force of 100 t hydraulic servo cylinder when the output of the piston rod is in the fixed constraint. The load simulation servo system is composed of oil sources, overflow valve, servo valve, and 100 t hydraulic servo cylinder. The model is shown in Figure 6 which is built through adding hydraulic components in the library [20, 21]. When the load instruction is 30 t, the experiment and simulation response curves are shown in Figure 7. The result indicates that the load response is particularly fast and stable.

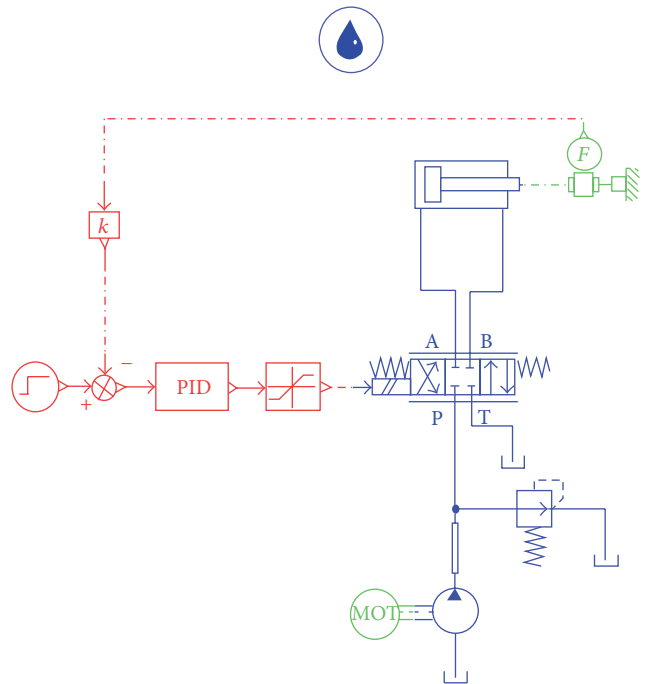


FIGURE 6: Model of load simulation system.

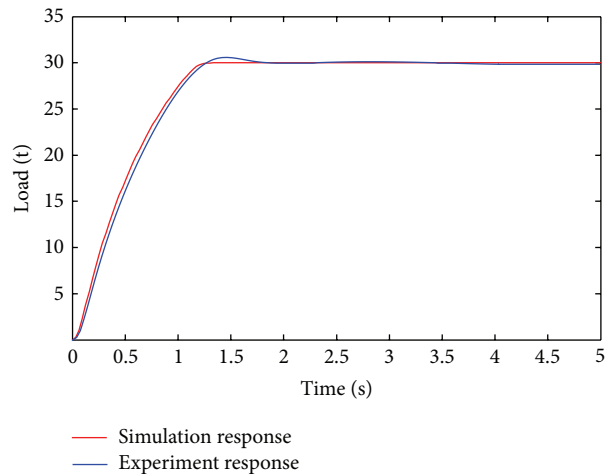


FIGURE 7: Response of the load simulation system.

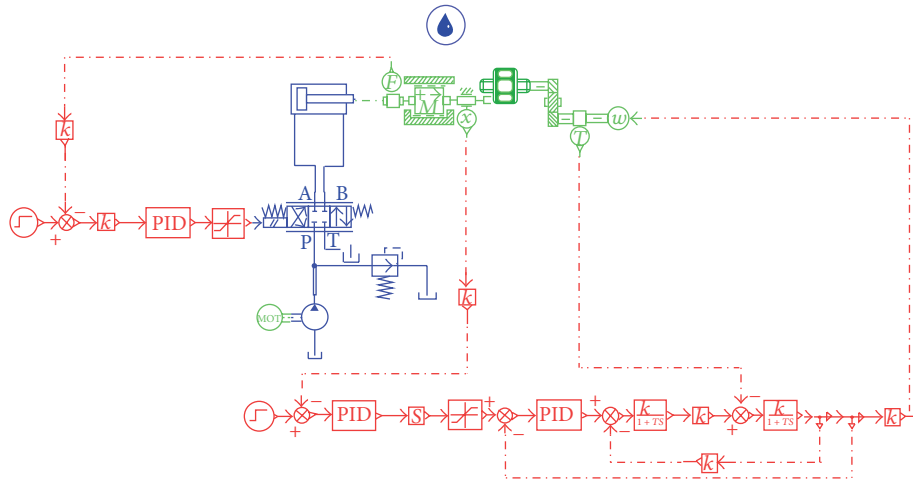


FIGURE 8: Model of the load simulator.

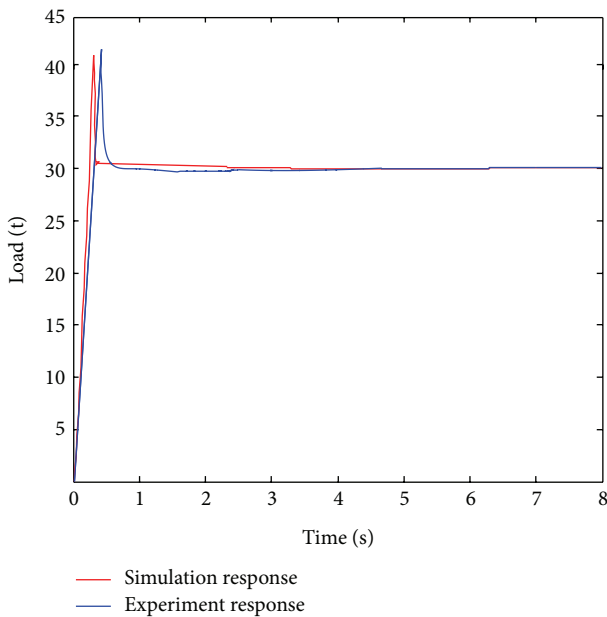


FIGURE 9: Response of the load.

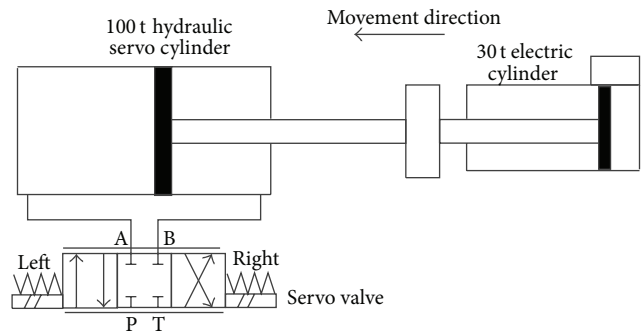


FIGURE 10: Schematic diagram of the load simulator.

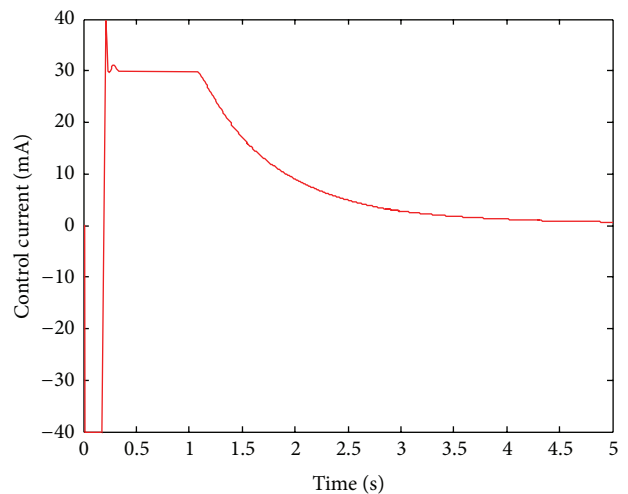


FIGURE 11: Control current.

3.3. *Modeling and Simulation of the Load Simulator.* Figure 8 shows the model of the load simulator through combining position servo system with load simulation system. Figure 9 shows the load responses curves when the position instruction is set to 100 mm and load instruction is set to 30 t. The result indicates that the model can reflect real system.

4. Reason of the Impact Load

Figure 10 is the schematic diagram of the load simulator. The control current of the servo valve is ± 40 mA. When the 30 t electric cylinder extends its piston rod along the movement direction and 100 t hydraulic servo cylinder provides 30 t load, the output of control current in the servo controller is shown in Figure 11. The control current is -40 mA in the initial stages of loading and servo valve core moves left in

order to provide 30 t load. P gets connected to A and B gets connected to T at this moment. The pressure of 100 t servo cylinder's rodless cavity is raised. Since 30 t electric cylinder extends its piston rod along the movement direction, the piston of 100 t servo cylinder is forced to move left.

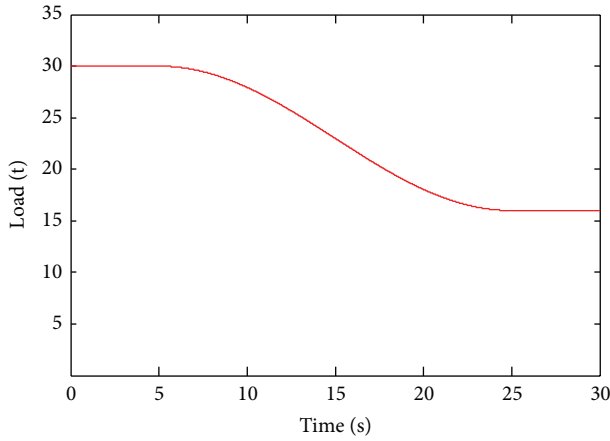


FIGURE 12: Control instruction of the 100 t servo cylinder.

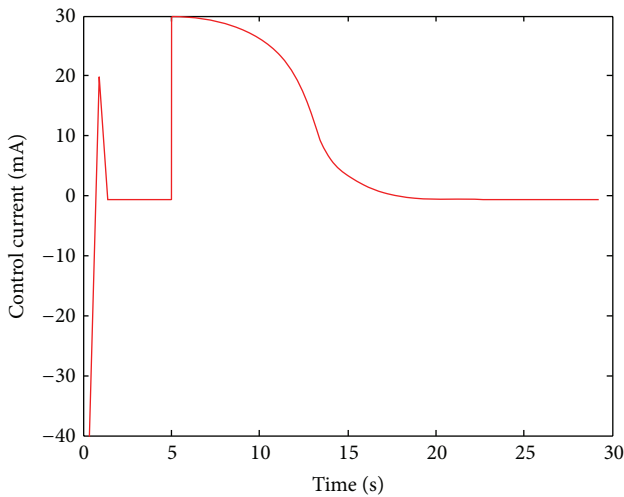


FIGURE 13: Control current.

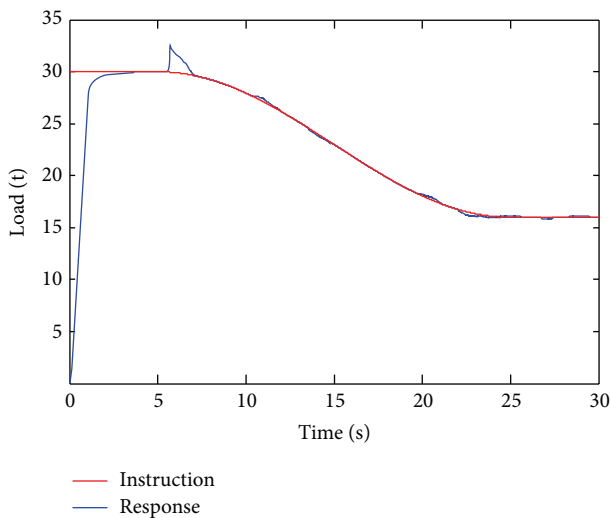


FIGURE 14: Load response of simulation.

The oil of A cannot be discharged by P, which makes the pressure of the rodless cavity rise in 100 t servo cylinder. The rod cavity will lead to negative pressure as B cannot suck oil by T. Therefore, the differential pressure between rodless cavity and rod cavity is expanding rapidly and the 40 t impact load appears in the initial stage. Then, the control current becomes positive value and servo valve core moves right to make P get connected to B and A get connected to T. The pressure of rodless cavity is kept by differential pressure between A and T, which can provide 30 t load. The instant rise and fall of control current will also produce impact load in the process of experiment because the servo valve works in the high pressure and large flow. Therefore, the changing rate of control current should not be too high.

5. Inhibition Methods of Impact Load

The impact load can seriously destroy the dynamic loading precision and even may damage the mechanical structure of electric cylinder, so we must adopt methods to suppress it. This paper presents some simple control algorithms based on structure invariance principle which is not only easily translated into computer language to be applied in the high precision real-time control system, but also can suppress the impact load.

5.1. Delay Control. The reason of initial impact load is the contradiction in movement direction between servo valve and 100 t servo cylinder. We present delay control method which changes the loading instruction through extending action time of 30 t loading (Figure 12). When the load reaches the scope of the loading precision, we start to issue control instructions of 30 t electric cylinder. The control current is shown in Figure 13. When 100 t servo cylinder completes loading, the control current becomes zero and servo valve core moves to the middle position. Then, the control current becomes positive value when 30 t electric cylinder starts to move, which makes the movement direction of valve core keep consistency with 100 t servo cylinder. It can be seen from load response of simulation in Figure 14 that the impact load is reduced to 32 t. Although the impact load is suppressed to a large extent, it lasts about two seconds in the initial stage of 30 t electric cylinder starting to move. Therefore, we present a control method of feedforward compensation based on speed.

5.2. Feedforward Compensation Based on Speed. The loading force is disturbed when 30 t electric cylinder starts to move. The feedforward compensation based on speed can improve dynamic tracking ability and restrain interference [22, 23]. The speed of 30 t electric cylinder multiplying by a scale factor will be a part of the control current of the servo valve. The new model of the load simulator is shown in Figure 15. When we apply these two methods into control program of the real system, the load response in the experiment is shown in Figure 16. It can be seen that when 100 t servo cylinder and 30 t electric cylinder start to be controlled, a small impact

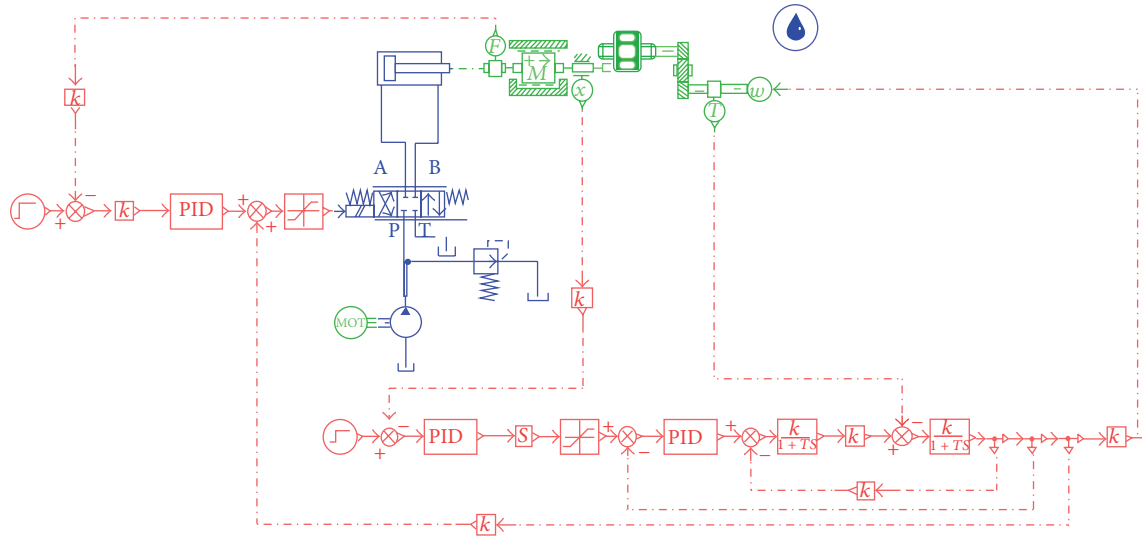


FIGURE 15: New model's load simulator.

load still exists. Therefore, we adopt a control method of incremental PID control algorithm.

5.3. Incremental PID Control Algorithm. The instant rise and fall of control current will also produce impact load in the process of experiment because the servo valve responds fast and works in the environment of high pressure and large flow. Therefore, the rate of control current should not be too high. The output of the incremental PID is $U(k)$ which can be achieved by the following:

$$U(k) = U(k-1) + \Delta U,$$

$$\Delta U = \Delta U_p + \Delta U_i + \Delta U_d,$$

$$\Delta U_p = K_p(\Delta e(k) - \Delta e(k-1)), \quad (2)$$

$$\Delta U_i = K_i(\Delta e(k) - \Delta e(k-1)) \times T,$$

$$\Delta U_d = \frac{K_d(\Delta e(k) - 2\Delta e(k-1) + \Delta e(k-2))}{T},$$

where K_p , K_i , and K_d are parameters of the PID algorithm, $\Delta e(k)$ is the difference between expected and sampling value, and T is the control period.

In order to improve the anti-interference ability of the system, we should not keep K_d zero. $\Delta e(k)$ is bigger and $\Delta e(k-1)$, $\Delta e(k-2)$ are both zero in the first control cycle and T is very small, which makes the value of $K_d(\Delta e(k) - 2\Delta e(k-1) + \Delta e(k-2))/T$ very big. Therefore, we should make $K_d = 0$ in the first control cycle and utilize adaptable value in the other control cycles.

When we adopt the above control methods, the load response of the load simulator in the experiment is shown in

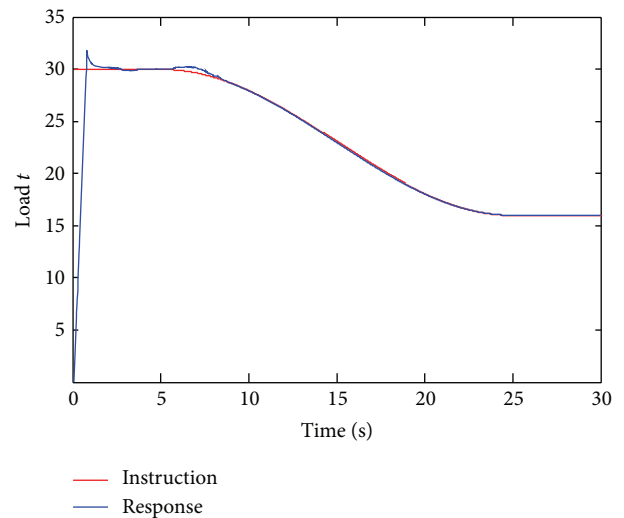


FIGURE 16: New model's load response in experiment.

Figure 17. It can be seen from Figures 2 and 17 that the impact load is suppressed in the process of dynamic loading.

6. Conclusion

The impact load of the large load simulator in the initial stage is caused by the contradiction in the direction of movement between servo valve and 100 t servo cylinder. The experiment result indicates that the combined application of delay control, feedforward compensation based on speed, and incremental PID control algorithm based on structural invariability principle not only improves the load environment, but also suppresses the impact load, which is

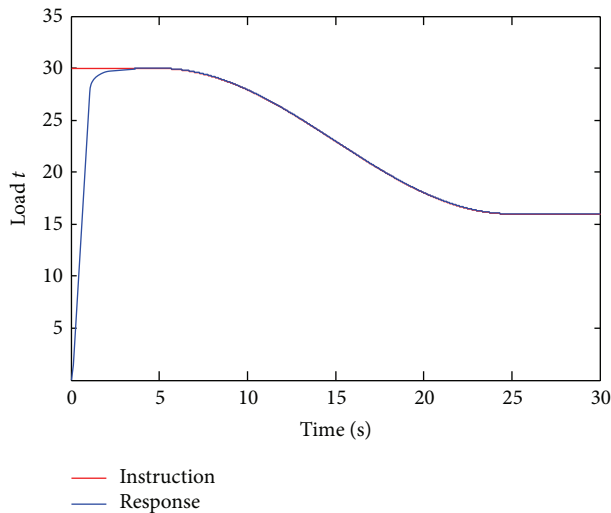


FIGURE 17: Response of the load simulator in experiment.

favorable for the application and generalization of the large load simulator.

Conflict of Interests

The authors declare that there is no conflict of interests regarding the publication of this paper.

References

- [1] W. Zhanlin, *Hydraulic Servo Control System*, Beihang University Press, Beijing, China, 1987.
- [2] Z. Jiao, Q. Hua, and X. Wang, "Evaluation system of load simulator," *Chinese Journal of Mechanical Engineering*, vol. 38, no. 11, pp. 26–30, 2002.
- [3] L. K. Stewart, B. Durantb, J. Wolfsonc, and G. A. Hegemierb, "Experimentally generated high-g shock loads using Hydraulic Blast Simulator," *International Journal of Impact Engineering*, vol. 6, no. 9, pp. 86–94, 2014.
- [4] D. H. Su and Y. Q. Wang, "Development of electro-hydraulic load simulator with high precise," in *Proceedings of the 5th International Conference on Fluid Power Transmission and Control*, pp. 281–285, Hangzhou, China, 2001.
- [5] C. W. Wang, Z. X. Jiao, S. Wu, and Y. X. Shang, "An experimental study of the dual-loop control of electro-hydraulic load simulator," *Chinese Journal of Aeronautics*, vol. 26, no. 6, pp. 1586–1595, 2013.
- [6] Y. Hao, L. Changchun, and C. Ce, "Simulation and experiment of electro—hydraulic servo systems load simulator," *Chinese Hydraulics and Pneumatics*, vol. 3, pp. 19–52, 2013.
- [7] K. Zhou, Y. Li, and Y. Yunfeng, "Research of the hydraulic load simulator control," *Science Technology and Engineering*, vol. 35, no. 12, pp. 9523–9527, 2012.
- [8] Z. Zhang, X. Liu, and J. Wang, "Robust H_{∞} sliding mode control with pole placement for a fluid power electrohydraulic actuator (EHA) system," *International Journal of Advanced Manufacturing Technology*, vol. 73, no. 5–8, pp. 1095–1104, 2014.
- [9] Z. Jiao, Q. Hua, X. Wang, and S. Wang, "Compound control of electro-hydraulic load simulator," *Chinese Journal of Mechanical Engineering*, vol. 38, no. 2, pp. 685–689, 2002.
- [10] H. Qing and J. Zongxia, "CRNN neural network control of the load simulator," *Chinese Journal of Mechanical Engineering*, vol. 38, no. 1, pp. 15–19, 2003.
- [11] Z. Jiao and Q. Hua, "RBF neural network control on electro-hydraulic load simulator," *Chinese Journal of Mechanical Engineering*, vol. 39, no. 1, pp. 10–14, 2003.
- [12] Z. Yuan and L. Wang, "Compound compensator based on cerebellar model articulation controller for surplus torque in passive electric loading system," *Journal of Tongji University*, vol. 32, no. 5, pp. 685–689, 2004.
- [13] L. Chenggong, J. Hongtao, and J. Zongxia, "Mechanism and suppression of extraneous torque of motor driver load simulator," *Journal of Beijing University of Aeronautics and Astronautics*, vol. 32, no. 2, pp. 204–208, 2006.
- [14] H. Zhang and S. Yang, "On energy-to-peak filtering for nonuniformly sampled nonlinear systems: A Markovian Jump System Approach," *IEEE Transactions on FUZZY System*, vol. 22, no. 1, pp. 212–222, 2014.
- [15] H. Zhang, X. Zhang, and J. Wang, "Robust gain-scheduling energy-to-peak control of vehicle lateral dynamics stabilization," *Vehicle System Dynamics*, pp. 309–338, 2014.
- [16] X. Wencan, "Electric cylinder and air cylinder," *Hydraulics Pneumatics & Seals*, vol. 24, no. 2, pp. 18–22, 2006.
- [17] T. Ying, "The analysis on driving and force of electric cylinder," *Heavy Machinery Science and Technology*, vol. 13, no. 1, pp. 10–14, 2007.
- [18] X. Xie and H. Yang, "Model of servo motor in the position servo system," *Journal of Beijing Institute of Technology*, vol. 16, no. 3, pp. 323–326, 1996.
- [19] F. Yongling, *Modeling and Simulation Based on AMESim*, Beihang University Press, Beijing, China, 2006.
- [20] M. Changlin, H. Xianxiang, and H. Lin, "Simulation and optimization studies of electro-hydraulic servo system based on AMESim," *Hydraulics Pneumatics & Seals*, vol. 1, pp. 32–34, 2006.
- [21] W. Yafeng and G. Jun, "Research on simulation technique based on AMESim for aircraft hydraulic system," *Journal of Shenyang University of Technology*, vol. 29, no. 4, pp. 368–371, 2007.
- [22] H. Zhang and J. Wang, "Combined feedback-feedforward tracking control for networked control systems with probabilistic delays," *Journal of the Franklin Institute, Engineering and Applied Mathematics*, vol. 351, no. 6, pp. 3477–3489, 2014.
- [23] Z. Shuai, H. Zhang, J. Wang, and J. Li, "Lateral motion control for four-wheel-independent-drive electric vehicles using optimal torque allocation and dynamic message priority scheduling," *Control Engineering Practice*, pp. 55–66, 2014.



Hindawi

Submit your manuscripts at
<http://www.hindawi.com>

